Building facade evaluation using instance segmentation on thermal images

Gerda Cones, Fiona C. Collins and Florian Noichl
Chair of Computational Modeling and Simulation, Technical University of Munich, Arcisstraße 21, 80333 Munich, Germany
E-mail(s): gerda.cones@tum.de, fiona.collins@tum.de, florian.noichl@tum.de

Abstract: To advance building energy efficiency assessments, Deep Learning (DL) technologies such as image segmentation can be leveraged to expedite evaluations. Previous research has applied instance segmentation to compute U-values of doors, walls, windows and facades, or has applied semantic segmentation to identify thermal anomalies. This work focused on training a DL instance segmentation model on a rudimentary dataset to discern and categorize different facade elements, including windows, doors, walls, floors, and thermal anomalies. The fine-tuned Mask RCNN ResNet-50+FPN model yielded the following segmentation Average Precision (AP) values: 45.6 (mean AP), 65.2 (window glazing), 53.5 (window), 34.9 (wall) and 17.2 (thermal bridge). The bounding box AP for thermal bridges, 28.6, highlights the model's ability to detect thermal bridges. The results presented in this paper indicate the potential for applying DL instance segmentation to thermal images to identify thermal bridges and estimate U-values using the Infrared Thermovision Technique (ITT). The dataset can be found in https://github.com/gerdac/thermal-images-instance.

Keywords: Thermal performance assessment, deep learning, instance segmentation, dataset

Erschienen in Tagungsband 35. Forum Bauinformatik 2024, Hamburg, Deutschland, DOI: 10.15480/882.13553

1 Introduction

The demand for accurate, rapid and accessible thermal performance assessments of buildings is becoming increasingly larger due to the urgency for efficient buildings. Thermography is being employed to evaluate buildings' envelopes and identify building defects' role on energy performance [1]. A critical factor in understanding heat loss is thermal transmittance, expressed as U-value, which can be determined using theoretical and in-situ methods [2]. However, it is not possible to develop accurate numerical models without knowing the internal structure [3]. Therefore, in-situ building inspections necessitate non-destructive investigations [4] to determine thermal bridging performance [3]. It is crucial to account for thermal bridges' higher heat losses while assessing the building's envelope thermal performance [3]. This work is based on a proof of concept for the integration of Infrared Thermovision Technique (ITT), a non-destructive quantitative infrared thermography (QIRT) technique developed by Albatici, Tonelli, and Chiogna [5] to calculate U-values, and Deep Learning (DL) image segmentation for analyzing thermal images as an approach for enhancing building thermal

performance assessments. This integration brings together the qualitative and quantitative aspects of infrared thermography. The work presented in this paper comprises the development of a rudimentary dataset, transfer learning and preliminary results for DL instance segmentation of windows, walls, doors and thermal bridges within thermal images.

2 Related Works

Infrared thermography is useful and time-efficient for in-situ assessment of the overall structure, especially for visible and invisible material defects, moisture and thermal failures [4]. When performing energy assessments, the determination of U-values is imperative [2]. The most widely used methods for U-value determination are the theoretical method, the heat flow meter (HFM) method, the simple hot box-heat flow meter method (SHB-HFM), the thermometric method (THM) and QIRT [2]. QIRT methods use infrared thermography to measure surface temperature, emissivity and reflected temperature [2]. ITT is a QIRT technique for determining U-values and employing the quantitative aspect of infrared thermographhy.

The automation of the qualitative aspect of infrared thermography through image segmentation rises as a possibility thanks to deep learning. However, the ground truth for thermal anomaly segmentation are subject to the potential subjective interpretation of thermographers and the difficulty of establishing definitive boundaries for different anomaly types [6]. One anomaly can be annotated by one expert as a single anomaly, while another expert may separate it into multiple anomalies [6]. This is likely a contributing factor to why image segmentation has not been extensively implemented on thermal images of buildings.

Instance segmentation was employed in the work of Sadhukhan, Peri, Sugunaraj, *et al.* [7] to develop a data-driven three-layered framework to calculate the heat-loss or U-values. Transfer learning was employed on approximately 500 thermal images from campus buildings at the University of North Dakota to train a Mask R-CNN model. The Average Precision (AP) at confidence level 0.50 was 0.67 for windows and 0.46 for facades. The mean Average Precision (mAP) was 0.56. The detection of windows outperformed that of facades, but the mask accuracy as evaluated by IoU was significantly more accurate for facades than windows; the IoUs were 0.50 and 0.05, respectively. To calculate the U-values, the manually annotated thermal images were used instead of the masks obtained from the Mask R-CNN model. Cumulative U-value calculations were used. [7]

3 Methodology

Accurate U-value calculations and comprehensive thermal analysis of building facades hinge upon the ability to precisely segment and classify individual components within thermal images. The methodology focuses on creating a specialized dataset for training the model to detect and categorize critical facade elements, such as walls, windows, and thermal anomalies, to accurately estimate U-values.

A dedicated dataset of thermal images collected under controlled weather conditions was manually labeled to train the model. The instance segmentation approach utilizes state-of-the-art tools such as Detectron2 and employs transfer learning strategies to expedite the training process.

Figure 1 depicts the envisioned DL-based approach. The approach is the following: thermal images are used as input for a DL image segmentation model, which results in instance masks for windows, walls, and thermal anomalies. The masks are then visualized for confirmation. These instance masks are then processed using weather and emissivity data to calculate U-values employing the ITT. This work comprises the mentioned steps up to the instance visualization.

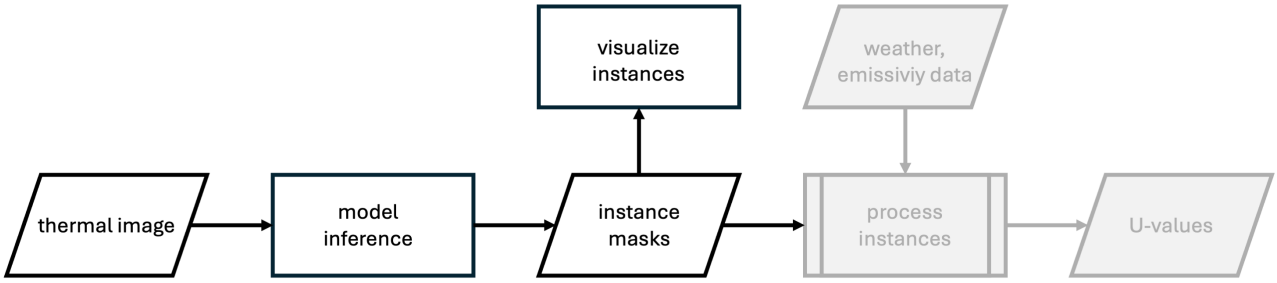

Figure 1: Proposed DL-based Approach for U-value calculation using thermal images. Greyed-out steps are not developed in this work.

3.1 Collection of Thermal Images for Dataset Development

To develop the dataset, weather.com was used to check whether the predicted weather conditions adhered to the 24 hours and 12 hours requirements and recommendations outlined in table 1, which tabulates the weather condition requirements and recommendations outlined in [5], [8]–[11]. Adherence to the recommendations and requirements is imperative, as stated in [8] moisture on the wall, radiant heat exchange, and solar radiation can render the values obtained using the thermograph unreliable. Especially with very porous materials, as the thermal conductance of materials is strongly influenced by temperatures and moisture conditions [12]. During collection, a FLIR A50 camera was used to collect thermal radiometric images over the course of two days. The sensors and data loggers listed in table 2 were utilized to confirm the weather condition during collection was as per table 1.

Table 1: Thermal Images Collection Requirements and Recommendations

Collection conditions	**24 hours before**	**12 hours before**	**During collection**
Overcast skies	▤ [8]	■ [5]	■
No solar radiation	-	▤ [9], [10]	■ [5]
Dry facade	-	-	■ [5], [8], [11]
$\Delta T = T_{int} - T_{out} > \frac{3}{U}$	■ [9]	■	■
$\Delta T \geq 5$℃	■ [9]	■	■
$\Delta T \geq 10$℃	▤ [10]	▤	▤
$\Delta T \leq \pm 30\%$	▤ [10]	▤	▤
$\Delta T_{int} \leq \pm 2$℃	-	-	■ [9]–[11]
$\Delta T_{out} \leq \pm 5$℃	-	-	■ [9], [11]
$\Delta T_{out} \leq \pm 10$℃	■ [11]	■ [11]	-
Hourly $\overline{v} \leq 5$m/s	■ [5]	■	-
$v \leq 0.5$m/s	-	-	■ [5]

Recommendations ▤ and Requirements ■.

Table 2: Equipment list

Equipment	Data collected
FLIR A50 camera (serial number 89800406)	thermal, RGB and MSX images
anemometer (turbulence testo probe)	wind speed, absolute pressure (m/s, hPa)
hygrometer (humidity/temperature testo probe)	humidity, temperature (%RH, °C)
thermometer (globe testo probe Ø 5.9")	temperature (°C)
testo data logger and software	logs data from testo probes
pyranometer (LICOR LI-200R)	solar radiation (W/m^2)
LICOR light sensor logger with GPS	GPS coordinates and logs pyranometer data

3.2 Dataset Development

After collecting the thermal images, the images were labelled using V7Labs' online data training platform, V7 Darwin, from v7labs.com. V7Lab's Darwin is an AI data engine that facilitates the labelling process using auto-annotate models. The process is the following: input data, create a workflow, establish the classes, check the data quality and export the labelled data. The classes were: wall, thermal bridge, window (glazing, frame), door (panel, frame), floor, other, foliage, and sky. The classes foliage and sky were discarded and not included in model training.

3.3 Model Training and Transfer Learning

The model training and transfer learning was performed in Google's Colaboratory notebooks. The methodology encompassed the following steps. First, Detectron2 [13] was installed and the Detectron2 utilities required were imported. The labelled dataset was pulled directly from V7 Darwin. Then the training, validation and testing splits were established and registered. The training data was then visualized to ensure the labels and metadata were correct. The Detectron2's default trainer's configurations were updated. The Mask RCNN R50-FPN 3x, trained on COCO Instance Segmentation, was chosen as the pre-trained model weights from Detectron2's Model Zoo [13]. A data augmentation program employing transformations to increase variability during the training process was implemented using a custom trainer by modifying the DatasetMapper. The specific transformations applied were: RandomCrop, RandomBrightness, RandomContrast, RandomSaturation, RandomLighting, and RandomFlip. Detectron2's COCOEvaluator [13] was then used to evaluate the models' metrics during training on the training and validation splits. Ultimately, the model was evaluated on the testing split.

4 Results

This section delineates the dataset development and inference performance results. Specifics regarding the dataset are outlined and the parameters and benchmarking results of the model are investigated.

4.1 Dataset Development

During a 2-day dataset collection period, 577 thermal, 118 RGB, and 114 MSX images were taken of various buildings within the borough of Maxvorstadt, Munich, Germany. The locations are mapped in fig. 2. From these 577 thermal images, several were of the same facade, or from buildings with very

similar construction structures. Therefore, a reduced amount of images were labelled, as the quantity and variety provided by the total dataset could be emulated using data augmentation. Therefore, the following criteria were implemented when filtering the images for labelling. Firstly, images of each building inspected were chosen for labelling, to provide the largest variety of window, door, and wall configurations. The second criterion was using images with several instances to provide highly variable training images when cropping transformations were applied. Thirdly, to improve the class balance, several images containing only walls and thermal bridges were also labelled. The thermal images were labelled using V7 Darwin. The final classes distribution can be seen in table 3, and the labelled and unlabelled images can be found in https://github.com/gerdac/thermal-images-instance.

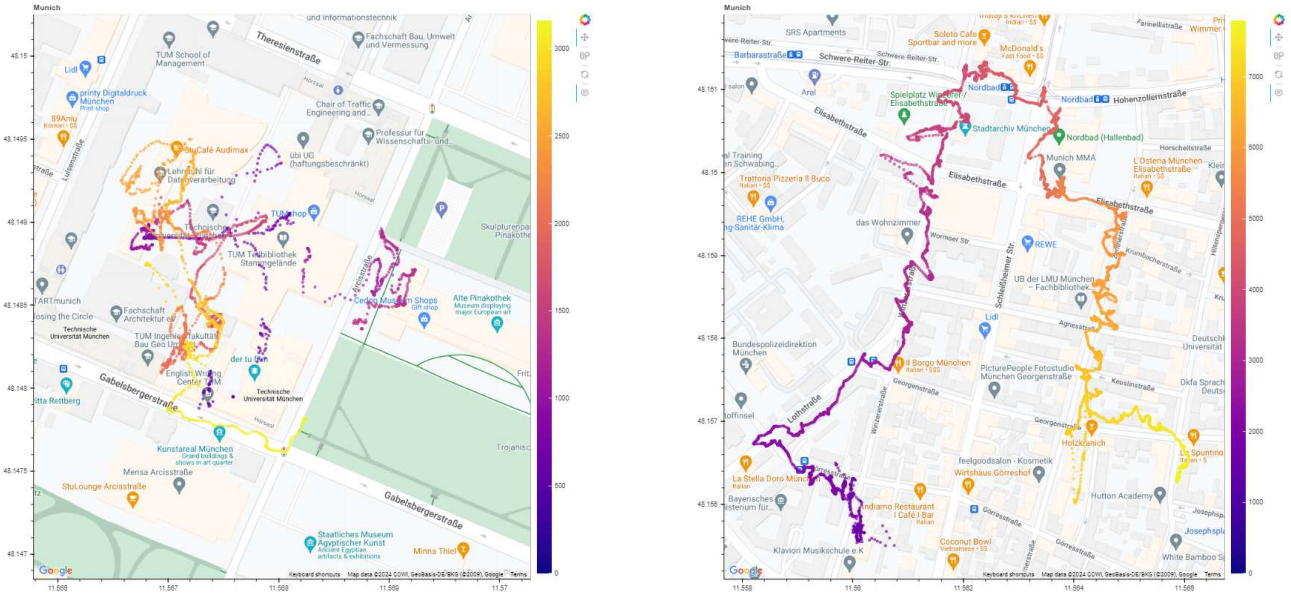

(a) GPS locations day 1.

(b) GPS locations day 2.

Figure 2: GPS locations during dataset collection

4.2 Inference Performance

The training hyperparameters used are outlined in table 4, and the AP and AP50 metrics for bounding boxes and segmentation masks are tabulated in table 5. The model demonstrated adequate detection precision to facilitate image segmentation, enabling U-value calculations directly from the segmentation masks, provided no foreign objects for which the model was not extensively trained on were in the foreground. However, the model was unable to identify all thermal bridges in the images. For the thermal bridge above and below the central window in fig. 3 (a), it was likely due to the dispersed appearance of the thermal bridge. The model should have been able to identify the parking sign and the thermal bridges under the top left window due to their stark contrast against the wall. However, due to the undersized training dataset, the model is only able to confidently identify sections of the facade and specific thermal bridges. Lowering the confidence threshold yielded different masks for the thermal bridges and the parking sign, as illustrated in fig. 3. Although lowered thresholds compromise the reliability of precise U-value calculations, the potential for employing differentiated thresholds for thermal bridges warrants consideration, given their irregular shapes and the importance of their

accurate detection in comprehensive building facade analysis. Furthermore, the segm/AP50 values were compared against [7], a related instance segmentation works focused on detecting the following building elements: doors, roofs, facades, beams and windows. Sadhukhan, Peri, Sugunaraj, *et al.* [7] presented AP25, AP50, and AP75 values for windows, facades, and their average in Table 12 of their study. Their model achieved AP50 values of 0.67 and 0.46 for windows and facades, respectively [7]. Comparatively, the model exhibited superior performance in these classes. However, AP values for the remaining classes were not disclosed, likely stemming from class imbalance challenges given the inherent ratio of windows and doors in buildings. This imbalance complicates the model's training process by biasing the more frequently represented classes, which affects the precision and recall of less common classes. [7] encountered similar challenges in detection accuracy, resorting to using their manually annotated images for the U-value calculations of the windows, walls and roofs.

Table 3: Class Distribution

	Label Classes	Instances
1	wall	169
2	thermal bridge	344
3	window	389
	a glazing	796
	b frame	275
4	door	16
	a panel	12
	b frame	13
5	floor	23
6	other	165

Table 4: Training Hyperparameters

Hyperparameter	Value
Training split	75%
Validation split	15%
Testing split	10%
Batch	4
Learning rate	0.0005
Iterations	4000
Regions of interest	128

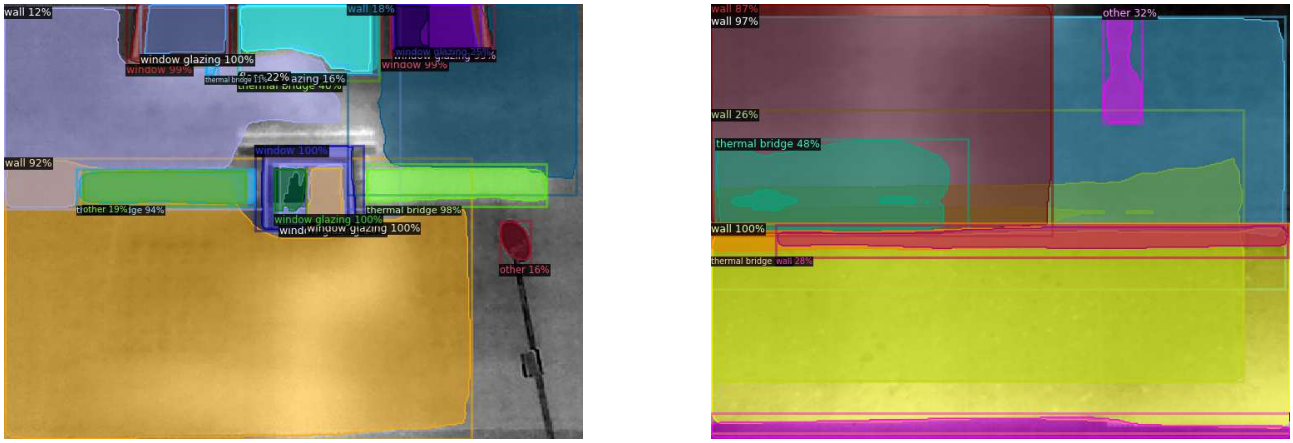

(a) Inference with 10% threshold

(b) Inference with 20% threshold

Figure 3: Segmented images at 10 m using different threshold levels.

5 Outlook

The future of thermal performance assessments could be based on non-intrusive U-value calculations or the identification of thermal bridges using deep learning instance segmentation. To enhance the

Table 5: AP values for bounding box and segmentation per class

Class	bbox/AP	bbox/AP50	segm/AP	segm/AP50
wall	39.7	67.1	34.9	50.4
thermal bridge	28.6	43.7	17.2	40.1
window	58.5	86.1	53.5	79.5
window glazing	61.3	92.8	65.2	92.8
window frame	0.0	0.0	0.0	0.0
door	70.0	100.0	80.0	100.0
door panel	80.0	100.0	80.0	100.0
door frame	0.0	0.0	0.0	0.0
floor	90.0	100.0	90.0	100.0
other	47.9	85.1	45.1	66.5

accuracy of the approach, improvements to the class balance and the implementation of panoptic segmentation could be pursued.

Improving the balance of the classes is a key factor for improving the model. For a fully functioning robust model all aspects of a facade should be included. Additionally, the instances labelled "other" were in fact different types of objects that are typically present in front of a facade. For future models, it could be beneficial to separate these items even further, or to leverage existing models that can identify these common items such as bikes, cars, people, and light fixtures.

For thermal bridges with dispersed heat loss and amorphous shapes, integrating instance and semantic segmentation, as in panoptic segmentation, offers a promising approach to delineating various facade elements while simultaneously flagging the presence of thermal bridges. Panoptic segmentation's dual capability to classify both discrete objects and amorphous regions, could be particularly effective for implementing the thermal bridge-specific Anomaly Identification Metric as developed by Kakillioglu, Masri, Pan, *et al.* [6], which severs the one-to-one instance dependency associated with instance segmentation. Leveraging the semantic component of the panoptic model to label pixels as thermal anomalies, irrespective of their sizes and shapes, while achieving accurate segmentation of building facade elements, has the potential to result in a robust model for thermal inspections.

6 Conclusion

This work contributes significantly to the advancement of building energy efficiency through the development of a rudimentary database to fine-tune an existing DL instance segmentation Mask RCNN ResNet-50+FPN backbone model for the analysis of thermal images. The model yielded the following AP values: 45.6 (mAP), 65.2 (window glazing), 53.5 (window), 34.9 (wall) and 17.2 (thermal bridge). The bounding box AP for thermal bridges, 28.6, suggests the model is able to detect thermal bridges but struggles with their amorphous shapes. This work sets the foundation for implementing DL instance segmentation on thermal images to identify thermal bridges and compute U-values using ITT.

References

[1] T. Rakha, Y. E. Masri, K. Chen, E. Panagoulia, and P. D. Wilde, “Building envelope anomaly characterization and simulation using drone time-lapse thermography”, *Energy and Buildings*, vol. 259, Mar. 2022. DOI: 10.1016/j.enbuild.2021.111754.

[2] D. Bienvenido-Huertas, J. Moyano, D. Marín, and R. Fresco-Contreras, *Review of in situ methods for assessing the thermal transmittance of walls*, Mar. 2019. DOI: 10.1016/j.rser.2018.12.016.

[3] M. O’Grady, A. A. Lechowska, and A. M. Harte, “Application of infrared thermography technique to the thermal assessment of multiple thermal bridges and windows”, *Energy and Buildings*, vol. 168, pp. 347–362, Jun. 2018. DOI: 10.1016/J.ENBUILD.2018.03.034.

[4] A. Tavukçuoğlu, “Non-destructive testing for building diagnostics and monitoring: Experience achieved with case studies”, *MATEC Web of Conferences*, vol. 149, p. 01 015, 2018. DOI: 10.1051/matecconf/201814901015.

[5] R. Albatici, A. M. Tonelli, and M. Chiogna, “A comprehensive experimental approach for the validation of quantitative infrared thermography in the evaluation of building thermal transmittance”, *Applied Energy*, vol. 141, pp. 218–228, Mar. 2015. DOI: 10.1016/j.apenergy.2014.12.035.

[6] B. Kakillioglu, Y. E. Masri, C. Pan, *et al.*, “A performance metric for the evaluation of thermal anomaly identification with ill-defined ground truth”, in *EG-ICE 2021 Workshop on Intelligent Computing in Engineering, Proceedings*, 2021, pp. 401–410.

[7] D. Sadhukhan, S. Peri, N. Sugunaraj, *et al.*, “Estimating surface temperature from thermal imagery of buildings for accurate thermal transmittance (u-value): A machine learning perspective”, *Journal of Building Engineering*, vol. 32, 2020. DOI: 10.1016/j.jobe.2020.101637.

[8] G. Dall’O’, L. Sarto, and A. Panza, “Infrared screening of residential buildings for energy audit purposes: Results of a field test”, *Energies*, vol. 6, pp. 3859–3878, 8 2013. DOI: 10.3390/en6083859.

[9] *Thermal Performance of Buildings-Qualitative Detection of Thermal Irregularities in Building Envelopes-Infrared Method*, BS EN 13187:1999. London, UK, May 1999.

[10] *Thermal insulation — Qualitative detection of thermal irregularities in building envelopes — Infrared method*, ISO 6781:1983(E). Switzerland, 1983.

[11] D. Bienvenido-Huertas, R. Rodríguez-Álvaro, J. J. Moyano, F. Rico, and D. Marín, “Determining the u-value of facades using the thermometric method: Potentials and limitations”, *Energies*, vol. 11, 2 Feb. 2018. DOI: 10.3390/en11020360.

[12] G. Ficco, F. Iannetta, E. Ianniello, F. R. D. Alfano, and M. Dell’Isola, “U-value in situ measurement for energy diagnosis of existing buildings”, *Energy and Buildings*, vol. 104, pp. 108–121, Jul. 2015. DOI: 10.1016/j.enbuild.2015.06.071.

[13] Y. Wu, A. Kirillov, F. Massa, W.-Y. Lo, and R. Girshick, *Detectron2*, https://github.com/facebookresearch/detectron2, 2019.